Multi-Stream Distributed Co-Phasing

Ribhu Chopra, *Student Member, IEEE*, Chandra R. Murthy, *Senior Member, IEEE*,
and Ramesh Annavajjala, *Senior Member, IEEE*

Abstract—In this paper, we develop a distributed co-phasing (DCP) technique for physical layer fusion of multiple data streams in a wireless sensor network with multiple destination nodes (DNs). The DNs can either be connected to a fusion center (referred to as centralized data processing; CDP) or process data independently and communicate with each other via a rate limited link (referred to as distributed data processing; DDP). In the first stage of this two-stage co-phasing scheme, sensors estimate the channel to the DNs using pilot symbols transmitted by the latter; following which they simultaneously transmit multiple streams of data symbols by pre-rotating them according to the estimated channel phases to the different DNs. The achievable rates for both CDP and DDP are derived to quantify the gains obtainable by multi-stream DCP. In order to aid data detection at the receiver, we propose a least squares based iterative algorithm for blind channel estimation in CDP-DCP. Following this, we develop a message passing based blind channel estimation algorithm for DDP-DCP. It is found using Monte Carlo simulations that for the CDP system, the proposed blind channel estimation algorithm achieves a probability of error performance very close to that with perfect CSI at the DNs, while using only a moderate number of unknown data symbols for channel estimation. We also derive approximate expressions for the error probability performance of the proposed system for both CDP and DDP and validate their accuracy using Monte Carlo simulations.

Index Terms—Distributed co-phasing, data fusion, MIMO, blind channel estimation, message passing, distributed data detection

I. INTRODUCTION

A. Motivation

In many wireless sensor network (WSN) applications, data fusion from multiple sensors observing a phenomenon is an important problem [2], [3]. Here, a set of distributed sensor nodes (SNs) need to wirelessly send their common data to one or more destination nodes (DNs) located far away. Distributed transmit beamforming, and in particular, distributed co-phasing (DCP), is a physical layer technique that can be used to provide coherent combining gain as well as spatial diversity gain for data fusion in WSNs [4]. In DCP, multiple transmitting nodes form a virtual antenna array to cooperatively send their data to the DNs. DCP also enjoys the benefits of requiring a fixed power transmission from the nodes, is robust to channel estimation errors, and it's feasibility in practical implementation is well established [5]. Further, DCP is inherently secure: when multiple nodes transmit their data such that it coherently combines over the channel at a given destination, it gets incoherently combined at any

R. Chopra and C. R. Murthy are with the Indian Institute of Science, Bangalore, India. R. Annavajjala is with the Charles Stark Draper Laboratory, Cambridge, MA, USA. Emails: ribhu@outlook.com, cmurthy1@gmail.com, ramesh.annavajjala@gmail.com. This work has appeared in part in [1].

unintended receiver, thereby making it hard to decode the data. This work focuses on the problem of simultaneously transmitting multiple data streams to a set of DNs using DCP.

In DCP, the communication between the SNs and DNs occurs in two stages. In the first stage, the DNs transmit known pilot symbols to the SNs in a round robin fashion, using which the SNs estimate the channels between themselves and the DNs. In the second stage, the SNs synchronously transmit their data to the DNs by pre-rotating the data by the estimated channel phase, thereby achieving coherent combining of the data intended to each destination at the respective node. Such a transmission scheme works when the channel is quasi-static and reciprocal [5], [6]. Transmission of pilots from the DNs, rather than the SNs, has multiple advantages: it saves power at the SNs; the DNs are typically connected to the mains and are capable of transmitting pilots at higher power than the energy-starved SNs; and it is more efficient in terms of training duration overhead when there are a significantly larger number of sensors compared to destinations. However, the key issue that occurs when multiple SNs simultaneously transmit their data to the different DNs via DCP is the inter-stream interference. The analysis and compensation of the inter-stream interference under both distributed and centralized processing at the DNs is the main focus of this paper.

B. Related Work

The problem of coherent communication from multiple distributed transmitted antennas to a distant receive antenna was first studied in [3], where a master slave architecture was proposed to synchronize the clocks of the distributed antennas under nonfading channels. The nonfading channel model studied in [3] was extended to fading channels in [5]. Distributed transmit beamforming (DTB) systems require carrier frequency synchronization across the SNs; its feasibility was experimentally demonstrated in [5] and [7]. Once carrier frequency synchronization has been achieved, the SNs need to transmit their data to the DNs in accordance with the DTB scheme. DTB requires accurate knowledge of the channels at the SNs. However, the effect of imperfect channel estimates on DTB schemes is studied in [8]. Feedback based approaches for DTB involving random and deterministic phase perturbations in the data sent by the DNs are studied in [6] and [9], respectively, and their convergence is studied in [10]. The problem of DTB has also been studied in the context of relay power allocation when multiple relays communicate with a base station in [11]. In [12], the authors propose to use DTB in a cellular system with a multi-antenna base station receiver and a single-antenna user terminal. Multi-antenna fusion centers for WSNs are considered in [13] and [14]. Asymptotic results

are derived to show the effect of multiple antennas on a WSN system in the presence of sensing and channel noise under both full and phase only CSI at the sensors in [13]. In [14], the authors compare the performance of two different decision fusion schemes for a MIMO WSN system.

In [15], the BER performance of DCP with BPSK modulation is compared against that of maximum ratio transmission, censored transmission, and truncated channel inversion. It is assumed in [15] that the CSI is not estimated at the fusion center (FC), and therefore, the comparison is limited to constant modulus constellations such as M-PSK. DCP is extended to non-constant modulus constellations in [16], and it is shown that higher order constellations can increase the rate achievable per channel use. Moreover, [16] also develops the notion of *channel corruption* for DCP systems to analytically characterize the flooring in the error performance due to channel estimation errors. All these works study DCP for a single DN system; our focus in this paper is on the scenario where the SNs wish to send multiple streams of data to multiple DNs, with each SN having a single transmit antenna.

C. Contributions

In the present work, we generalize the single DN model to a case where the SNs transmit independent data to multiple DNs. The DNs can either be connected to a central processing entity similar to a FC, or each DN may possess processing capabilities and be connected to the other DNs via a rate-limited channel. These setups are referred to as centralized data processing-DCP (CDP-DCP) and distributed data processing-DCP (DDP-DCP), respectively. It is important to note that it is not possible to pre-rotate the data so as to coherently combine at multiple DNs simultaneously, since the channels to the different DNs are independent.

The main objective of the present manuscript is *to devise schemes for collaboratively transmitting K common data streams that are available at all the sensor nodes to K corresponding destination nodes, as well as analyze their performance*. For this purpose we propose and analyze *multi-stream DCP* (MS-DCP), where the nodes transmit multiple independent data streams with each stream co-phased to coherently combine at a different DN. The main contributions of this work are as follows:

1) We derive the statistics of the effective MIMO channel matrix arising due to MS-DCP with multiple DNs. (See Section II.)
2) We compare the information rates achievable by MS-DCP against single-stream DCP (SS-DCP) for both CDP and DDP. The gains observed further motivate the need to study the design and analysis of DCP based schemes with multiple DNs. (See Section III.)
3) Inspired by the significant performance improvement achievable even in the absence of CSI at the DNs, we develop an iterative blind algorithm for channel estimation at the DNs for CDP-DCP. (See Section IV.)
4) Motivated by the significant gap between performance of CDP-DCP and DDP-DCP, we develop a message passing based channel estimation algorithm for interference mitigation at the receivers. (See Section V.)
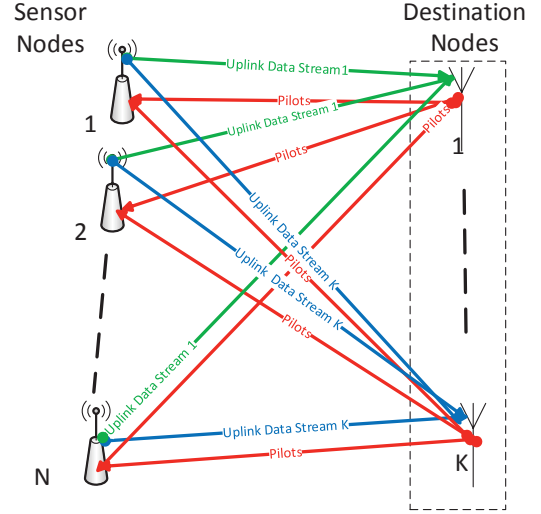

Figure 1.   The proposed system model with multiple DNs.

5) We derive approximate analytical expressions for the probability of symbol error for both CDP-DCP and DDP-DCP with M-PSK signaling. (see Section VI.)
6) Via detailed simulations, we prescribe the recommended system parameters such as the data and pilot signal-to-noise ratio (SNR), the number of DNs, and the number of sensor nodes to achieve a desired rate and reliability. (See Section VII.)

Therefore, MS-DCP along with the proposed blind channel estimation algorithms is a strong candidate for reliable and energy efficient data fusion in WSNs. Also, the proposed blind channel estimation algorithms can be relevant in joint data detection and channel estimation for other channels with known signal structures.

Notation: Boldface lowercase and uppercase letters represent vectors and matrices, respectively. The kth column and row of $\mathbf{A}$ are denoted by $\mathbf{a}_k$, and $\mathbf{a}^{(k)}$, respectively. $(.)^H$ represents the Hermitian operation on a vector or a matrix, whereas $(.)^T$ denotes the transpose operation. $\|\cdot\|_2$ and $\|\cdot\|_F$ respectively represent the ℓ_2 norm of a vector and the Frobenius norm of a matrix. $E[\cdot]$ and $\text{var}(\cdot)$ represent the mean and variance of a random variable.

II. SYSTEM MODEL AND CHARACTERIZATION OF THE CHANNEL STATISTICS

We consider N distributed SNs that wish to transmit common data to K DNs. The DNs can either be connected to an FC, or individually possess processing capabilities and be connected to each other via a rate-limited channel. The system model is illustrated in Fig. 1.

In DCP, communication between the SNs and the DNs takes place in two time division duplexed stages. In the first stage, each of the K DNs broadcast M_p pilot symbols in a round robin fashion. These pilots are used by the N SNs to estimate

the coefficients of the NK channels between themselves and the DNs. In the second stage, all the SNs simultaneously transmit their common data to the DNs for the next M_d channel uses. It is assumed that the channel coherence time exceeds $M = KM_p + M_d$ symbols [4], [5], and that the channels between the DNs and the SNs are reciprocal [15]. Note that, with the proposed DCP scheme, coherent combining at the DNs can be achieved only if the channels exhibit reciprocity. In addition, it is assumed that the SNs are carrier and frequency synchronized. It has been noted in [4] that the phase of such a system once synchronized remains in sync for durations much longer than the channel coherence time, and therefore the cost of synchronization is not considered in this work. The training signal received by the lth SN during channel uses $(k-1)M_p + 1$ through kM_p, $k = 1, \ldots, K$, can be written as

$$
\begin{aligned}
y_l[n] &= \alpha_{k,l} e^{j\theta_{k,l}} \sqrt{\mathcal{E}_p} + w_l[n] \\
&\qquad n = (k-1)M_p + 1, \ldots, kM_p
\end{aligned} \tag{1}
$$

where $\mathcal{E}_p$ is the pilot power of the DNs, $\alpha_{k,l}$ is the Rayleigh distributed channel gain with $E[|\alpha_{k,l}|^2] \triangleq \Omega_{k,l}$, $\theta_{k,l}$ is the uniformly distributed channel phase between the kth DN and the lth SN and $w_l[n]$ is the zero mean circularly symmetric complex additive white Gaussian noise with per dimension variance $\frac{N_0}{2}$.

The maximum likelihood (ML) estimate of the phase of the kth DN at the lth SN is [15]

$$
\widehat{\theta}_{k,l} = \tan^{-1} \left(\frac{\sum_{n=(k-1)M_p+1}^{kM_p} \Im\{y_l[n]\}}{\sum_{n=(k-1)M_p+1}^{kM_p} \Re\{y_l[n]\}} \right) \tag{2}
$$

where $\Re\{.\}$ and $\Im\{.\}$ denote the real and imaginary parts of a complex number, respectively. After estimating the channel phases for each of the K DNs, sensor l transmits $x_l[n]$, such that

$$
x_l[n] = \sum_{i=1}^{K} s_i[n] e^{-j\widehat{\theta}_{i,l}} \quad n = KM_p + 1, \ldots, M, \tag{3}
$$

where $s_i[n]$ is the nth modulation symbol over the ith stream, assumed to be the same for all the transmitting nodes (i.e., fully-correlated sensing field), and independent across the streams. The transmit power of each SN is assumed to be $\mathcal{E}_s$, such that

$$
\mathcal{E}_s = E[|x_l[n]|^2] = KE[|s_i[n]|^2]. \tag{4}
$$

The second equality arises from the assumption that all the streams are allotted the same amount of power. During the data transmission stage, the received signal on kth DN is

$$
\begin{aligned}
y_k[n] &= \sum_{l=1}^{N} \alpha_{k,l} e^{j\theta_{k,l}} x_l[n] + v_k[n], n = KM_p + 1, \ldots, M \\
&= N \sum_{i=1}^{K} h_{ki} s_i[n] + v_k[n] \\
&= N h_{kk} s_k[n] + N \sum_{l=1, l\neq k}^{K} h_{kl} s_l[n] + v_k[n]
\end{aligned} \tag{5}
$$

where $v_k[n]$ is the zero mean circularly symmetric complex Gaussian noise at the kth DN with a per dimension variance $\frac{N_0}{2}$, and

$$
h_{ki} = \frac{1}{N} \sum_{l=1}^{N} \alpha_{k,l} \exp\left(j \left[\theta_{k,l} - \widehat{\theta}_{i,l}\right]\right) \tag{6}
$$

is the effective channel between the ith data stream transmitted from the N SNs to the kth DN. Note that h_{ki} is unknown at the DNs. In a matrix-vector notation, (5) can equivalently be expressed as

$$
\mathbf{y}[n] = N\mathbf{H}\mathbf{s}[n] + \boldsymbol{v}[n], \tag{7}
$$

with $\mathbf{y}[n] = [y_1[n]\, y_2[n] \ldots y_K[n]]^T$, $\mathbf{s}[n] = [s_1[n]\, s_2[n] \ldots s_K[n]]^T$, $\mathbf{v}[n] = [v_1[n] \ldots v_K[n]]^T$, and $\mathbf{H} \in \mathcal{C}^{K \times K}$, with its (k, i)th element h_{ki} as defined above.

A. Channel Matrix Under Perfect DCP

To characterize the statistical properties of the channel matrix $\mathbf{H}$, let us first consider the case with perfect DCP, i.e., $\widehat{\theta}_{k,l} = \theta_{k,l}$. In this case, the diagonal entries of the channel matrix can be written as $h_{kk} = \frac{1}{N} \sum_{l=1}^{N} \alpha_{k,l}$, where $\alpha_{k,l}$ are independent Rayleigh distributed random variables (r.v.s).

The (k, i)th off-diagonal entry, $k \neq i$, is $h_{ki} = \frac{1}{N} \sum_{l=1}^{N} \alpha_{k,l} \exp\left(j\left[\theta_{k,l} - \theta_{i,l}\right]\right)$. As both $\theta_{k,l}$ and $\theta_{i,l}$ are uniformly distributed, therefore, their difference also has a uniform distribution. Hence, the (k, i)th entry, $k \neq i$, of the effective channel matrix is a zero mean complex Gaussian r.v. with variance $\frac{1}{N^2} \sum_{l=1}^{N} \Omega_{k,l}$.

B. Channel Matrix Under Imperfect DCP

At finite pilot SNR, the phase estimate $\widehat{\theta}_{k,l}$ is imperfect. The error in the phase estimate between the kth DN and the lth sensor node is $\widetilde{\theta}_{k,l} \triangleq \theta_{k,l} - \widehat{\theta}_{k,l}$. In this case, the diagonal entries of the channel matrix can be written as

$$
h_{kk} = \frac{1}{N} \sum_{l=1}^{N} \alpha_{k,l} \exp(j\widetilde{\theta}_{k,l}). \tag{8}
$$

For the analysis to follow, we will need the first two moments of the entries of the entries of the effective DCP channel matrix $\mathbf{H}$. These can be worked out, following the procedure presented in [16], as follows:

$$
E[\alpha_{k,l} \cos(\widetilde{\theta}_{k,l})] = \sqrt{\frac{\Omega_{k,l}\pi}{4}} \sqrt{\frac{\Omega_{k,l}\xi}{1 + \Omega_{k,l}\xi}}, \tag{9}
$$

where $\xi \triangleq \frac{M_p \mathcal{E}_p}{N_0}$ is the downlink pilot SNR. Also,

$$
E[\alpha_{i,k} \sin(\widetilde{\theta}_{k,l})] = 0. \tag{10}
$$

Therefore,

$$
E[h_{kk}] = \frac{1}{N} \sum_{l=1}^{N} \sqrt{\frac{\Omega_{k,l}\pi}{4}} \sqrt{\frac{\Omega_{k,l}\xi}{1 + \Omega_{k,l}\xi}}. \tag{11}
$$

Further,

$$
E[|h_{kk}|^2] = \frac{1}{N^2} \sum_{l=1}^{N} \Omega_{k,l} \left(1 + \sum_{m=1, m\neq l}^{N} \frac{\pi}{4} \cdot \frac{\Omega_{k,m}\xi}{1 + \Omega_{k,m}\xi} \right), \tag{12}
$$

and therefore,

$$\text{var}(h_{kk}) = \frac{1}{N^2}\sum_{l=1}^{N}\Omega_{k,l}\left[1 - \frac{\pi}{4}\left(\frac{\Omega_{k,l}\xi}{1+\Omega_{k,l}\xi}\right)\right]. \quad (13)$$

Similarly, for the off-diagonal terms,

$$
\begin{aligned}
E[h_{ki}] &= \frac{1}{N}\sum_{l=1}^{N}E[\alpha_{k,l}\exp(j(\theta_{k,l}-\hat{\theta}_{i,l}))] \\
&= 0 \quad (14)
\end{aligned}
$$

and

$$
\begin{aligned}
\text{var}(h_{ki}) &= \frac{1}{N^2}\left(\sum_{l=1}^{N}E[\alpha_{k,l}^2] \right. \\
&\quad + \left. \sum_{m=1,m\neq l}^{N}\left|E[\alpha_{k,l}\exp(j(\theta_{k,l}-\hat{\theta}_{i,l}))]\right|^2\right) \\
&= \frac{1}{N^2}\sum_{l=1}^{N}\Omega_{k,l}. \quad (15)
\end{aligned}
$$

In the above discussion, we have assumed that the entries of the channel matrix between the SNs and the DNs are independent and non-identically distributed. This leads to complicated expressions for the first and second order statistics of the effective channel matrix. In order to simplify these, we assume in the remainder of this paper that the channels between the SNs and the DNs are independent and identically distributed (i.i.d.) such that $E[|\alpha_{k,l}|^2] = \Omega$. Consequently, the moments of the channel matrix can be written as

$$E[h_{kk}] = \sqrt{\frac{\Omega\pi}{4}}\sqrt{\frac{\xi\Omega}{1+\xi\Omega}}, \quad (16)$$

$$E[|h_{kk}|^2] = \frac{1}{N}\Omega\left(1 + (N-1)\frac{\pi}{4}\frac{\xi\Omega}{1+\xi\Omega}\right), \quad (17)$$

$$\text{var}(h_{kk}) = \frac{1}{N}\Omega\left[1 - \frac{\pi}{4}\left(\frac{\xi\Omega}{1+\xi\Omega}\right)\right], \quad (18)$$

and

$$\text{var}(h_{ki}) = \frac{\Omega}{N}, \quad i \neq k. \quad (19)$$

The expressions for first two orders of channel statistics for the i.i.d. and i.n.d. cases are tabulated in Table I. In the next section, the achievable data rates for both CDP-DCP and DDP-DCP are analyzed to show that a larger number of streams in a DCP based communication system leads to significantly improved achievable data rates compared to the SS-DCP case due to the spatial multiplexing of multiple data streams.

III. Mutual Information Analysis of Multistream DCP

In this section, we derive the asymptotically achievable data rates between the SNs and the DNs to quantify the potential improvement in data rates that can be achieved by using multiple data streams in DCP.

We start with the signal model in (7):

$$\mathbf{y}[n] = N\mathbf{H}\mathbf{s}[n] + \mathbf{v}[n]. \quad (20)$$

The received signal covariance matrix for a given realization of the channel matrix $\mathbf{H}$ is hence given as

$$
\begin{aligned}
\mathbf{R}_{yy|\mathbf{H}} &\triangleq E[\mathbf{y}[n]\mathbf{y}^H[n]|\mathbf{H}] \\
&= N^2\mathbf{H}\mathbf{R}_{ss}\mathbf{H}^H + N_0\mathbf{I}_K, \quad (21)
\end{aligned}
$$

where $\mathbf{R}_{ss} \triangleq E[\mathbf{s}[n]\mathbf{s}^H[n]]$ is the transmit signal covariance matrix. For independent data streams, this can be expressed as $\mathbf{R}_{ss} = \frac{\mathcal{E}_s}{K}\mathbf{I}_K$. The achievable data rate for this channel with a Gaussian codebook is therefore

$$R^{\text{CDP}}(\mathbf{H}) = \log_2\left(\det\left(I_K + \frac{N^2\mathcal{E}_s}{KN_0}\mathbf{H}\mathbf{H}^H\right)\right). \quad (22)$$

Letting $\mathbf{\Psi} \triangleq \mathbf{H}\mathbf{H}^H$, the kth diagonal element of $\mathbf{\Psi}$ is

$$
\begin{aligned}
\psi_{kk} &= \sum_{i=1}^{K}|h_{ki}|^2 \\
&= |h_{kk}|^2 + \sum_{i=1;i\neq k}^{K}|h_{kl}|^2 \\
&= \frac{1}{N^2}\sum_{l=1}^{N}\alpha_{k,l}^2 \\
&\quad + \frac{1}{N^2}\sum_{l,m=1;l\neq m}^{N}\alpha_{k,l}\alpha_{k,m}e^{j(\tilde{\theta}_{k,l}-\tilde{\theta}_{k,m})} \\
&\quad + \sum_{i=1;i\neq k}^{K}\left(\frac{1}{N^2}\sum_{l=1}^{N}\alpha_{il}^2 \right. \\
&\quad + \left. \sum_{l,m=1;m\neq l}^{N}\alpha_{k,l}\alpha_{k,m}e^{j(\theta_{k,l}-\theta_{k,m}-\hat{\theta}_{i,l}+\hat{\theta}_{i,m})}\right). (23)
\end{aligned}
$$

For large N and K, using the law of large numbers, the above expression concentrates around its mean with high probability, and is given as

$$
\begin{aligned}
\psi_{kk} &\approx \frac{1}{N^2}NE[\alpha_{kl}^2] + \frac{(K-1)}{N^2}NE[\alpha_{il}^2] \\
&\quad + \frac{1}{N^2}N(N-1)E^2[\alpha_{k,l}e^{j\tilde{\theta}_{k,l}}] \\
&\quad + \frac{K-1}{N^2}N(N-1)E^2[\alpha_{k,l}e^{j(\theta_{k,l}-\tilde{\theta}_{i,l})}]. \quad (24)
\end{aligned}
$$

Hence, ψ_{kk} can be approximated by its deterministic equivalent

$$\psi_{kk} \approx \frac{1}{N}\left(K\Omega + (N-1)\frac{\pi}{4}\times\frac{\xi\Omega^2}{1+\xi\Omega}\right). \quad (25)$$

Defining $c \triangleq \frac{K}{N}$, the limiting value of ψ_{kk} becomes

$$\lim_{N\to\infty}\psi_{kk} = \Omega\left(c + \frac{\pi}{4}\times\frac{\xi\Omega}{1+\xi\Omega}\right). \quad (26)$$

Similarly, the (k,q)th element of $\mathbf{\Psi}$ can be expressed as

$$\psi_{kq} = \sum_{i=1}^{K}h_{ki}h_{qi}^*. \quad (27)$$

This is a zero mean r.v. with variance proportional to $\frac{K^2}{N^4}$. Consequently, its limiting value can be approximated as

$$\lim_{N\to\infty}\psi_{kq} \approx 0. \quad (28)$$

Table I
EQUIVALENT CHANNEL STATISTICS FOR I.I.D. AND I.N.D. CHANNELS

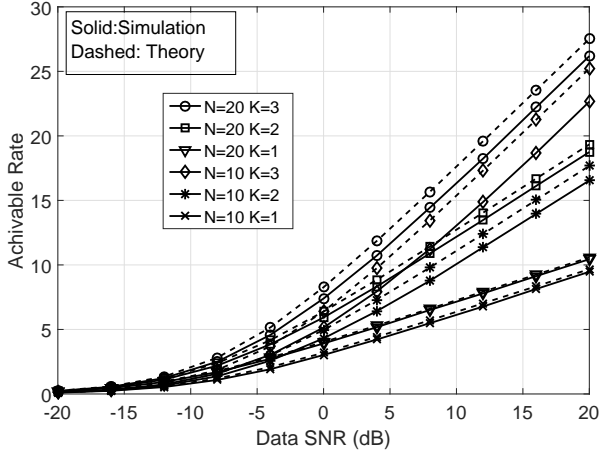|	i.n.d.	i.i.d.
$E[h_{kk}]$	$\frac{1}{N}\sum_{l=1}^{N}\sqrt{\frac{\Omega_{k,l}\pi}{4}}\sqrt{\frac{\Omega_{k,l}\xi}{1+\Omega_{k,l}\xi}}$	$\sqrt{\frac{\Omega\pi}{4}}\sqrt{\frac{\xi\Omega}{1+\xi\Omega}}$
$E[|h_{kk}|^2]$	$\frac{1}{N^2}\sum_{l=1}^{N}\Omega_{k,l}\left(1+\sum_{m=1,m\neq l}^{N}\frac{\pi}{4}\times\frac{\Omega_{k,m}\xi}{1+\Omega_{k,m}\xi}\right)$	$\frac{1}{N}\Omega\left(1+(N-1)\frac{\pi}{4}\frac{\xi\Omega}{1+\xi\Omega}\right)$
$E[h_{ki}]$	0	0
$E[|h_{ki}|^2]$	$\frac{1}{N^2}\sum_{l=1}^{N}\Omega_{k,l}$	$\frac{1}{N}\Omega$

Figure 2. Comparison of achievable rates for DCP with different number of streams (K), for $N = 20$ sensors.

Substituting (25) and (28) in (22), we can express the achievable rate independently of the channel matrix realization as

$$R^{\text{CDP}} = K\log_2\left(1+\frac{N^2\mathcal{E}_s}{KN_0}\left(c\Omega+\frac{\pi}{4}\frac{\xi\Omega^2}{1+\xi\Omega}\right)\right). \quad (29)$$

Defining $\bar{\eta}_0 \triangleq \frac{N\Omega\mathcal{E}_s}{N_0}$ as the effective data SNR, the achievable rate for large N and K becomes

$$R^{\text{CDP}} = K\log_2\left(1+\frac{1}{c}\left(c+\frac{\pi}{4}\frac{\xi\Omega}{1+\xi\Omega}\right)\bar{\eta}_0\right). \quad (30)$$

Now, for sufficiently large data and pilot SNR, the above can be approximated as

$$R^{\text{CDP}} \approx K\log_2\left(1+\frac{1}{c}\left(c+\frac{\pi}{4}\right)\bar{\eta}_0\right). \quad (31)$$

Since $N \gg K$, and consequently $c \ll 1$, therefore,

$$R^{\text{CDP}} \approx K\log_2\left(1+\frac{\pi}{4c}\bar{\eta}_0\right). \quad (32)$$

This results in an SNR gain $\frac{\pi N}{4K}$, that grows with N and decreases with K. However, in (32), K appears both inside and outside the log term, resulting in a net increase in the achievable rate with K. In Fig. 2, we plot the achievable rates as a function of the effective data SNR (in dB) for different number of data streams (K) in a $N = 20$ sensor node CDP-DCP based system. It can be observed that the simulation results closely follow the derived results. At moderate to high SNR, the achievable rates grow almost linearly with the

number of streams. Thus, the use of multiple DNs can result in significantly higher rates in a CDP-DCP based system.

Next, we consider the DDP-DCP scheme. Recall that the received signal at the kth DN is given by (5). Defining $z_{k,l}[n] \triangleq Nh_{kl}s_l[n]$ as the interference in the kth stream due to the lth stream, the interference in the kth stream due to all the other streams can be written as $z_k[n] = \sum_{l\neq k} z_{k,l}[n]$.

Now, since the channel coefficients as well as the symbols sent over the different streams are zero mean i.i.d. r.v.s, we have $E[z_k[n]] = 0$, and

$$\begin{aligned} E\left[|z_k[n]|^2\right] &= (K-1)N^2E[|h_{kl}|^2]E[|s_l|^2] \\ &= (K-1)\frac{N\Omega\mathcal{E}_s}{K}. \end{aligned} \quad (33)$$

Hence, the interference power scales linearly with the number of SNs. The signal-to-interference-plus-noise-ratio (SINR) of the kth stream can therefore be expressed as

$$\eta_k = \frac{N\Omega\left(1+(N-1)\frac{\pi}{4}\frac{\xi\Omega}{1+\xi\Omega}\right)\frac{\mathcal{E}_s}{K}}{(K-1)\frac{N\Omega\mathcal{E}_s}{K}+N_0}. \quad (34)$$

Further simplification of (34) leads to

$$\eta_k = \frac{\left(\frac{1}{N}+\frac{N-1}{N}\frac{\pi}{4}\frac{\xi\Omega}{1+\xi\Omega}\right)}{\frac{(K-1)}{N}+\frac{K}{N\bar{\eta}_0}}. \quad (35)$$

With $c = \frac{K}{N}$, and for an asymptotically large number of SNs, η_k becomes

$$\eta_k = \frac{\frac{\pi}{4}\frac{\xi\Omega}{1+\xi\Omega}}{c\left(1+\frac{1}{\bar{\eta}_0}\right)}. \quad (36)$$

The corresponding asymptotic sum rate with K independent data streams can be written as

$$R^{\text{DDP}} = K\log_2\left(1+\frac{\frac{\pi}{4}\frac{\xi\Omega}{1+\xi\Omega}}{c(1+\frac{1}{\bar{\eta}_0})}\right). \quad (37)$$

Now, for large pilot SNR, ξ, and data SNR, $\bar{\eta}_0$, (36) reduces to $\frac{\pi}{4}\frac{N}{K}$. Consequently, the achievable rate in (37) reduces to $K\log_2\left(1+\frac{\pi}{4}\frac{N}{K}\right)$, which is the limiting rate for a DDP system. The achievable data rates for CDP-DCP and DDP-DCP based systems for 25 and 50 SNs and different numbers of DNs and hence different values of c are plotted in Fig. 3. Again, the simulated results are observed to closely follow the derived results.

The achievable data rates for CDP-DCP and DDP-DCP based systems for 25 and 50 SNs in case of an i.n.d. channel matrix are illustrated in Fig. 4. Here, the channel coefficients are assumed to be complex Gaussian distributed with variances
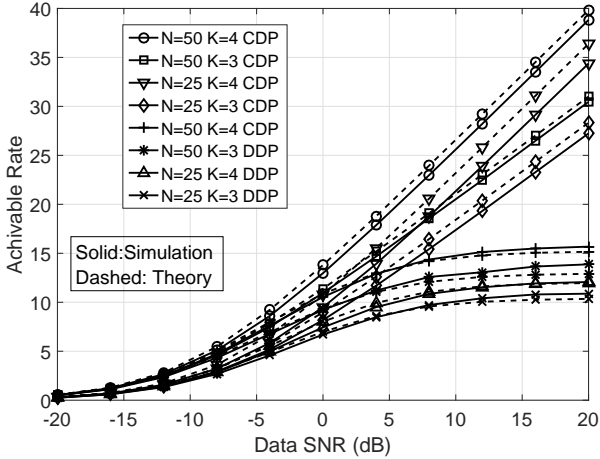
Figure 3. Comparison of achievable rates for CDP-DCP and DDP-DCP with different number of streams (K), for $N = 25$ and $N = 50$ sensors.
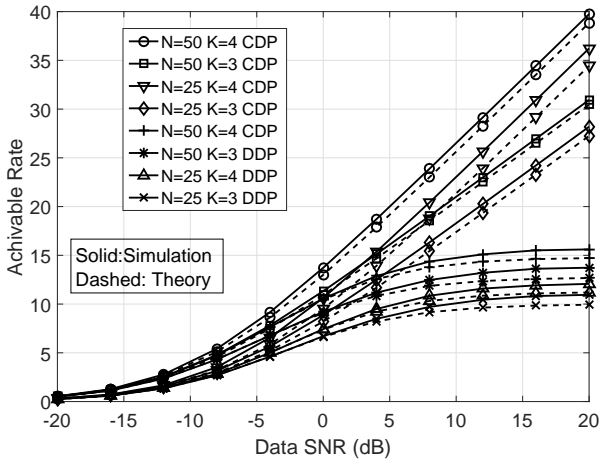

Figure 4. Comparison of achievable rates for CDP-DCP and DDP-DCP with different number of streams (K), for $N = 25$ and $N = 50$ sensors in an i.n.d channel.

depending on the path loss between the transmitting node and the receiving node. The SNs and DNs are assumed to be uniformly distributed over square regions with side 10m each. The centers of the two squares are assumed to be separated by 100m, and the path loss exponent is assumed to be 3. The path loss is normalized such that the path loss coefficient of the path connecting the center of the DN square to that of the SN square is unity. Using a similar procedure as the above, the approximate theoretical expressions for R^{CDP} and R^{DDP} can be obtained as

$$
R^{\mathrm{CDP}} = \sum_{k=1}^{K} \log_2 \left(1 + \frac{N^2 \mathcal{E}_s}{K N_0} \left(\sum_{l=1}^{N} \left(\sum_{i=1}^{K} \Omega_{i,l} \right. \right. \right.
$$
$$
\left. \left. \left. + \sum_{m=1;m\neq l}^{N} \frac{\xi \Omega_{k,m}}{1 + \xi \Omega_{k,m}} \right) \right) \right), \tag{38}
$$

$$
R^{\mathrm{DDP}} = \sum_{k=1}^{K} \log_2 \left(1 + \sum_{l=1}^{N} \frac{N^2 \mathcal{E}_s}{\sum_{i=1;i\neq k}^{K} \Omega_{i,l} \mathcal{E}_s + K N_0} \right.
$$
$$
\left. \times \left(\left(\Omega_{k,l} + \sum_{m=1;m\neq l}^{N} \frac{\xi \Omega_{k,m}}{1 + \xi \Omega_{k,m}} \right) \right) \right). \tag{39}
$$

It is observed for both i.i.d and i.n.d. cases at moderate to high data SNR, there is a significant difference between the achievable rates of CDP and DDP systems. This difference arises due to the fact that at moderate to high SNR the DDP-DCP based system becomes interference limited. This motivates us to look for interference mitigation techniques and the resultant information rates for multi stream DDP-DCP networks.

A. DDP-DCP with Mitigated Interference

In the above discussion, CDP-DCP represents the case where all the DNs have perfect knowledge of the interfering channel coefficients, and perfect information about the data sent over all the other streams, whereas DDP-DCP represents the case where the DNs neither have any information about the data received by the other DNs nor about the interfering channel coefficients. Here, we consider a general case where all the DNs have limited erroneous estimates of both the data received at the other DNs, as well as the interfering channel coefficients. This information can be used to mitigate inter-stream interference at different DNs, and hence improve the overall system performance.

The estimate of the coefficient of lth interfering stream at the kth DN, $\hat{h}_{kl}$, can be expressed as

$$
\hat{h}_{kl} = h_{kl} + \tilde{h}_{kl}, \tag{40}
$$

where $\tilde{h}_{kl}$ is the channel estimation error with zero mean and a variance $\sigma_{\tilde{h}}^2$. Similarly, the estimate of the symbol received by the lth node at the nth instant, and shared by all the nodes can be expressed as

$$
\hat{s}_l[n] = s_l[n] + \tilde{s}_l[n] \tag{41}
$$

with $\tilde{s}[n]$ being the zero mean symbol error independent of the transmitted symbol whose variance $\sigma_{\tilde{s}}^2$ is a function of the probability of symbol error over the lth stream, $P_{e,l}$, and the average transmit energy.

Using these, an estimate of the interference at the kth DN due to the lth stream can be expressed as

$$
\hat{z}_{k,l}[n] = N \hat{h}_{kl} \hat{s}_l[n]. \tag{42}
$$

Defining $\hat{z}_k[n] \triangleq \sum_{l=1,l\neq k}^{K} \hat{z}_{k,l}[n]$ as the total estimated interference, we can write the received signal with mitigated interference, $\hat{y}_k[n] \triangleq y_k[n] - \hat{z}_k[n]$, as

$$
\hat{y}_k[n] = N h_{kk} s_k[n] + \tilde{z}_k[n] + v_k[n], \tag{43}
$$

with $\tilde{z}_k[n] = z_k[n] - \hat{z}_k[n]$ as the residual interference whose lth component can be expanded as $\sum_{l=1,l\neq k}^{K} \tilde{z}_{k,l}[n]$ where

$$
\tilde{z}_{k,l}[n] = N h_{kl} s_l[n] - N \hat{h}_{kl} \hat{s}_l[n]. \tag{44}
$$

Substituting (40) and (41) in (44), we arrive at

$$
\tilde{z}_{k,l}[n] = -N(\tilde{h}_{kl} s_l[n] + h_{kl} \tilde{s}_l[n] - \tilde{h}_{kl} \tilde{s}_l[n]). \tag{45}
$$

Assuming channel and symbol errors to be independent, it follows that $E[\tilde{z}_{k,l}[n]] = 0$, and

$$
\begin{aligned}
E[|\tilde{z}_{k,l}[n]|^2] &= N^2 E[|h_{kl}|^2] E[|\tilde{s}_l[n]|^2] \\
&\quad + N^2 E[|\tilde{h}_{kl}|^2] E[|s_l[n]|^2] \\
&\quad + N^2 E[|\tilde{h}_{kl}|^2] E[|\tilde{s}_l[n]|^2].
\end{aligned}
\tag{46}
$$

But, $E[|\tilde{h}_{kl}|^2] = \sigma_{\tilde{h}}^2$ and $E[|\tilde{s}_l[n]|^2] = \sigma_{\tilde{s}}^2$. Therefore,

$$
E[|\tilde{z}_{k,l}[n]|^2] = \sigma_{\tilde{s}}^2 N\Omega + \frac{N^2 \sigma_{\tilde{h}}^2 \mathcal{E}_s}{K} + N^2 \sigma_{\tilde{h}}^2 \sigma_{\tilde{s}}^2.
\tag{47}
$$

Defining $\mu \triangleq \frac{E[|\tilde{z}_{k,l}[n]|^2]}{E[|z_{k,l}[n]|^2]}$ as the interference mitigation factor, we can write

$$
\mu = \frac{K \sigma_{\tilde{s}}^2}{\mathcal{E}_s} + \frac{\sigma_{\tilde{h}}^2}{\frac{\Omega}{N}} + \frac{K \sigma_{\tilde{h}}^2 \sigma_{\tilde{s}}^2}{\frac{\Omega}{N} \mathcal{E}_s}.
\tag{48}
$$

The first term in this equation corresponds to the ratio of the signal error power to the overall signal power. As shown in Appendix A, this term is of the order of the probability of symbol error and therefore much smaller than unity for a well designed system. The second term corresponds to the ratio of the channel estimation error to the channel gain. The channel estimation error for our proposed DDP scheme with interference mitigation is derived in Section V-A. At a moderate SNR and about $M_d = 200$ data symbols per frame, this term is at least one order of magnitude below unity (see Fig. 6). The third term being a product of the first two terms will also be much less than 1. Therefore, for moderate to high SNR, the value of μ can safely be bounded as $\mu \leq 1$.

Using this, the SINR of the received signal with mitigated interference can be expressed as

$$
\hat{\eta}_k = \frac{N^2 E[|h_{kk} s_k[n]|^2]}{E[|\tilde{z}_k[n]|^2] + E[|v_k[n]|^2]}.
\tag{49}
$$

From (17), and using $E[|\tilde{z}_k[n]|^2] = \mu E[|z_k[n]|^2]$, it can be shown that for a large number of sensor nodes, $\hat{\eta}_k$ is asymptotically approximated as

$$
\hat{\eta}_k = \frac{\frac{\pi}{4} \frac{\xi\Omega}{1+\xi\Omega}}{c \left(\mu + \frac{1}{\bar{\eta}_0} \right)}.
\tag{50}
$$

Therefore, the overall achievable data rate for transmission of K streams with DDP-DCP and mitigated interference becomes

$$
R^{\text{DDP-IM}} = K \log_2 \left(1 + \frac{\frac{\pi}{4} \frac{\xi\Omega}{1+\xi\Omega}}{c \left(\mu + \frac{1}{\bar{\eta}_0} \right)} \right).
\tag{51}
$$

This equation reduces to (30) for $\mu = 0$ and (37) for $\mu = 1$. Therefore, by accurately estimating the interference in a DDP-DCP based scheme, we can achieve information rates similar to a CDP-DCP based system. This motivates us to develop message passing based distributed channel estimation and data detection schemes for DDP-DCP in Section V.

B. Information Rates with Finite Symbol Constellations

In the above discussion, we derived the rates achievable using a Gaussian codebook. However, practical communication systems use finite symbol codebooks. Therefore, we now derive the mutual information achievable for CDP-DCP based systems with finite symbol constellations. We focus on the CDP-DCP based schemes here because they outperform the DDP-DCP based schemes. Moreover, as will be shown later, the performance of the DDP-DCP based systems can be made to approach that of the CDP-DCP based systems using limited-rate cooperation between the DNs via a message passing algorithm. Another benefit of considering the mutual information with finite constellations is that it allows us to study the effect of the lack of channel knowledge at the DNs on the achievable rates.

If the symbol constellation for each data stream is represented by $\mathcal{S}$, the overall symbol constellation for K streams is the Cartesian product $\mathcal{S}^K$ with each symbol having a probability mass $\frac{1}{|\mathcal{S}|^K}$. The MI of the system model discussed above can be evaluated with perfect, erroneous, or no channel knowledge at the DN cluster as follows [17]:

- With perfect CSI at the DN cluster

$$
\begin{aligned}
I^{\text{CSI}}(\mathbf{y}; \mathbf{s}) = E_{\mathbf{H}} \Bigg[&\sum_{\mathbf{s} \in \mathcal{S}^K} \frac{1}{|\mathcal{S}|^K} \int_{\mathbf{y} \in \mathcal{C}^K} p(\mathbf{y}|\mathbf{H}, \mathbf{s}) \\
&\log \frac{p(\mathbf{y}|\mathbf{H}, \mathbf{s})}{p(\mathbf{y}|\mathbf{H})} d\mathbf{y} \Bigg]
\end{aligned}
\tag{52}
$$

where $\mathcal{C}^K$ is the K dimensional complex field, and $E_{\mathbf{H}}$ represents the expectation over the distribution of the effective channel matrix. Due to the additive nature of noise, $p(\mathbf{y}|\mathbf{H}, \mathbf{s})$ is a K dimensional circularly symmetric complex Gaussian with mean $\mathbf{Hs}$ and a per dimension variance $\frac{N_0}{2}$. Also, $p(\mathbf{y}|\mathbf{H}) = \sum_{\mathbf{s} \in \mathcal{S}^K} \frac{1}{|\mathcal{S}|^K} p(\mathbf{y}|\mathbf{H}, \mathbf{s})$.

- With erroneous CSI at the DN cluster

$$
\begin{aligned}
I^{\text{est-CSI}}(\mathbf{y}; \mathbf{s}) = E_{\hat{\mathbf{H}}} \Bigg[&\sum_{\mathbf{s} \in \mathcal{S}^K} \frac{1}{|\mathcal{S}|^K} \int_{\mathbf{y} \in \mathcal{C}^K} p(\mathbf{y}|\hat{\mathbf{H}}, \mathbf{s}) \\
&\log \frac{p(\mathbf{y}|\hat{\mathbf{H}}, \mathbf{s})}{p(\mathbf{y}|\hat{\mathbf{H}})} d\mathbf{y} \Bigg].
\end{aligned}
\tag{53}
$$

Here, $\hat{\mathbf{H}}$ is the channel estimate at the DN cluster, such that $\hat{\mathbf{H}} = \mathbf{H} + \tilde{\mathbf{H}}$, with $\tilde{\mathbf{H}}$ being the channel estimation error. If we model the estimation error as complex Gaussian with variance depending on the training signal SNR, then, $p(\mathbf{y}|\hat{\mathbf{H}}, \mathbf{s})$ is zero mean circularly symmetric complex Gaussian, and $p(\mathbf{y}|\hat{\mathbf{H}}) = \sum_{\mathbf{s} \in \mathcal{S}^K} \frac{1}{|\mathcal{S}|^K} p(\mathbf{y}|\hat{\mathbf{H}}, \mathbf{s})$.

- With no CSI

$$
I^{\text{no-CSI}}(\mathbf{y}; \mathbf{s}) = \sum_{\mathbf{s} \in \mathcal{S}^K} \frac{1}{|\mathcal{S}|^K} \int_{\mathbf{y} \in \mathcal{C}^K} p(\mathbf{y}|\mathbf{s}) \log \frac{p(\mathbf{y}|\mathbf{s})}{p(\mathbf{y})} d\mathbf{y}
\tag{54}
$$

where $p(\mathbf{y}|\mathbf{s}) = E_{\mathbf{H}}[p(\mathbf{y}|\mathbf{H}, \mathbf{s})]$, and $p(\mathbf{y}) = \sum_{\mathbf{s} \in \mathcal{S}^K} \frac{1}{|\mathcal{S}|^K} p(\mathbf{y}|\mathbf{s})$

Closed form solutions for the above expressions are hard to obtain, we therefore use Monte Carlo simulations to evaluate them.
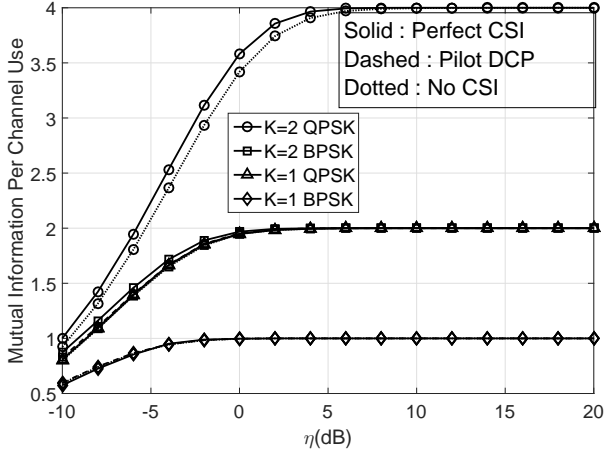
Figure 5. Comparison of mutual information for DCP with different amounts of channel knowledge at the DN cluster for different constellations and different number of DNs (K) and 10 SNs.

Fig. 5 plots the MI between 10 SNs and a DN cluster for different transmit constellations and numbers of DNs as a function of the transmit SNR (in dB). The average downlink pilot SNR for all these cases was assumed to be 10 dB. It can be seen that an increase in the number of DNs as well as in the constellation order results in improved information rates. Also, the use of larger constellations and a greater number of DNs improves the system performance when the CSI is imperfectly known or even unknown at the DN cluster. This motivates us to develop blind channel estimation techniques to recover both the transmitted symbols and estimate the CSI at the DNs to improve data detection performance without explicitly transmitting known pilot symbols from the power-starved SNs.

IV. BLIND CHANNEL ESTIMATION FOR CDP-DCP

It was shown above that higher order constellations and a larger number of DNs results in higher information rates for a CDP-DCP based system. However, in order to employ techniques such as ML detection or sphere decoding [18] on the received signal, the DNs need an estimate of the matrix channel $\mathbf{H}$.

There exists a substantial body of literature on blind channel estimation techniques, a good review of which can be found in [19], [20]. It can be observed that the effective channel matrix for the system model discussed in this paper has a special structure due to the diagonal entries being positive real numbers with high probability. This structure can be exploited to perform joint channel estimation and data detection without requiring any training symbols to be sent from the SNs to the DNs. In the sequel, we propose two blind channel estimation techniques for our system model.

A. Covariance Method

The finite sample approximate of the covariance matrix of the received signal for a channel realization $\mathbf{H}$ and M_d

received symbols can be defined as

$$\hat{\mathbf{R}}_{yy|\mathbf{H}} = \frac{1}{M_d} \sum_{n=KM_p+1}^{M} \mathbf{y}[n]\mathbf{y}^H[n]. \tag{55}$$

We can now define

$$\hat{\mathbf{P}}_{yy} = \hat{\mathbf{R}}_{yy|H} - N_0 \mathbf{I}_K, \tag{56}$$

such that,

$$E[\hat{\mathbf{P}}_{yy}] = N^2 \mathbf{H} E[\mathbf{ss}^H] \mathbf{H}^H. \tag{57}$$

Using the eigenvalue decomposition of $\hat{\mathbf{P}}_{yy}$, the effective DCP channel can be estimated as

$$\hat{\mathbf{H}} = \frac{1}{N} \hat{\mathbf{Q}}_y \hat{\mathbf{\Lambda}}_y^{1/2} \hat{\mathbf{Q}}_y^H (\mathbf{Q}_s \mathbf{\Lambda}_s^{1/2} \mathbf{Q}_s^H)^{-1} \tag{58}$$

where $\hat{\mathbf{Q}}_y$ and $\hat{\mathbf{\Lambda}}_y$ are, respectively, the $K \times K$ eigenvector and eigenvalue matrices of $\hat{\mathbf{P}}_{yy}$, and $\mathbf{Q}_s$ and $\mathbf{\Lambda}_s$ are the eigenvector and eigenvalue matrices of the transmitted signal covariance matrix $E[\mathbf{ss}^H]$. Note that the diagonal entries of the effective DCP matrix are real and positive with high probability. Therefore, only the real, positive square roots of the eigenvalues of $\hat{\mathbf{P}}_{yy}$ and $E[\mathbf{ss}^H]$ are considered for estimating $\hat{\mathbf{H}}$.

B. Iterative Minimization Based Method

Here, we present an iterative algorithm that works with multiple DNs. The joint ML estimate of the effective DCP channel and the transmitted data can be written as

$$(\hat{\mathbf{H}}, \hat{\mathbf{S}}) = \arg \min_{\mathbf{H}, \mathbf{S}} \|\mathbf{Y} - N\mathbf{H}\mathbf{S}\|_2 \tag{59}$$

where the matrices $\mathbf{Y}$ and $\mathbf{S}$ are defined as $\mathbf{Y} = [\mathbf{y}[KM_p + 1] \ldots \mathbf{y}[M]]$ and $\mathbf{S} = [\mathbf{s}[KM_p+1] \ldots \mathbf{s}[M]]$. Since the data and the channel matrices are independent, the above expression can be minimized iteratively with respect to each of these variables while keeping the other fixed. This problem can therefore be written as

$$\hat{\mathbf{s}}[n] = \arg \min_{\mathbf{s}[n] \in \mathcal{S}^K} \|\mathbf{Y} - N\hat{\mathbf{H}}\mathbf{s}[n]\|_2 \tag{60}$$

$$\hat{\mathbf{H}} = \arg \min_{\mathbf{H} \in \mathcal{C}^{K \times K}} \|\mathbf{Y} - N\mathbf{H}\hat{\mathbf{S}}\|_2. \tag{61}$$

Equation (60) can be viewed as a symbol detection problem for a MIMO receiver with a known channel matrix $\hat{\mathbf{H}}$. This can be solved via a search over the constellation $\mathcal{S}^K$ or via sphere decoding [18]. If a linear receiver is desired, one can compute, for a linear zero-forcing receiver, $\hat{\mathbf{S}} = \text{round}\left((\hat{\mathbf{H}}^H\hat{\mathbf{H}})^{-1}\hat{\mathbf{H}}^H\mathbf{Y}/N\right)$, where round(.) quantizes each entry of the matrix passed as the argument to the nearest constellation point. To find a minimizer for equation (61), we observe that the objective function is a convex function in $\mathbf{H}$. Differentiating it w.r.t. $\mathbf{H}$, setting the derivative to zero and solving, we obtain the well-known linear least-squares solution

$$\hat{\mathbf{H}} = \frac{1}{N} \mathbf{Y}\hat{\mathbf{S}}^\dagger, \tag{62}$$

where the superscript † represents the Moore-Penrose inverse of a matrix. The value of $\hat{\mathbf{H}}$ obtained in (58) could act as a reasonable initial estimate of $\mathbf{H}$ to solve (60). Then,

equations (61) and (60) can be solved iteratively to obtain estimates of the channel matrix as well as the transmitted symbols. A modified K-means algorithm was proposed for blind channel estimation with DCP in [16]. However, that algorithm is restricted to a single antenna at the FC, whereas the algorithm discussed above can be used to obtain a channel estimate for both single as well as multiple DN CDP-DCP based systems.

Convergence: The above algorithm alternately minimizes an objective function that is lower bounded by 0, with respect to the two variables $\mathbf{H}$ and $\mathbf{s}$. Further, the objective function is guaranteed to reduce in every iteration, since each sub-problem is solved optimally. Hence, the iterative procedure is guaranteed to converge to a local optimum. This is a characteristic shared by all the algorithms of this nature.

V. MESSAGE PASSING BASED BLIND CHANNEL ESTIMATION FOR DDP-DCP

It was observed in Section III that the DDP-DCP based system becomes interference limited for moderate to high SNR. However, the interference can be canceled out if each node is aware about the symbols received by the other nodes, along with the corresponding channel coefficients. It is shown in this section that a node can use the knowledge of the symbols sent to other nodes to estimate the channel coefficients for the corresponding streams. Since all streams of data but the kth constitute interference for the kth node, we can therefore use the knowledge of the signals sent over other streams to estimate the inter-stream interference at a given node. For this purpose, we develop a message passing [21] based blind channel estimation algorithm for joint channel estimation and data detection at the DNs. It is assumed that the nodes can exchange their decoded symbols over a rate-limited channel to allow the other nodes to estimate and subsequently subtract the inter stream interference. The received signal at the kth node can be written as

$$\mathbf{y}^{(k)} = N\mathbf{h}^{(k)}\mathbf{S} + \mathbf{v}^{(k)} \qquad (63)$$

where $\mathbf{y}^{(k)}$ and $\mathbf{h}^{(k)}$ represent the kth rows of $\mathbf{Y}$ and $\mathbf{H}$, respectively.

Defining $\mathbf{h}^{'(k)} = [h_{k1}, \ldots, h_{k(k-1)}, h_{k(k+1)}, \ldots, h_{kK}]$, $\mathbf{s}'_k[n] = [s_1[n], \ldots, s_{k-1}[n], s_{k+1}[n], \ldots, s_K[n]]$, and $\mathbf{S}^{'(k)} = \left[\left(\mathbf{s}'_k[1]\right)^T \ldots \left(\mathbf{s}'_k[M_d]\right)^T\right]$ we can express the inter stream interference as

$$\mathbf{z}^{(k)} = [z_k[1], \ldots, z_k[M_d]] = N\mathbf{h}^{'(k)}\mathbf{S}^{'(k)} \qquad (64)$$

where $\mathbf{S}^{'(k)} \in \mathcal{S}^{(K-1)\times M_d}$ is the matrix containing all but the kth stream of transmitted symbols. Then, (63) becomes

$$\mathbf{y}^{(k)} = N h_{kk}\mathbf{s}^{(k)} + \mathbf{z}^{(k)} + \mathbf{v}^{(k)}. \qquad (65)$$

Now, if the kth DN receives the estimates $\hat{\mathbf{S}}^{'(k)} = [\hat{\mathbf{s}}^{(1)T} \ldots \hat{\mathbf{s}}^{(k-1)T}\hat{\mathbf{s}}^{(k+1)T}\hat{\mathbf{s}}^{(K)T}]^T$, then the joint channel estimation and data detection problem can be formulated as

$$[\hat{\mathbf{h}}^{(k)}\hat{\mathbf{s}}^{(k)}] = \arg \min_{\mathbf{h}^{(k)},\mathbf{s}^{(k)}} \|\mathbf{y}^{(k)} - N\mathbf{h}^{'(k)}\hat{\mathbf{S}}^{'(k)} - N h_{kk}\mathbf{s}^{(k)}\|_2. \qquad (66)$$

Algorithm 1 Message passing based blind channel estimation for MS-DCP

Initialize: $i = 0$; $f_k = 1$;

$\hat{h}_{kk} = \left[\max\left(\frac{\frac{1}{M_d}\sum_{n=1}^{M_d}|y_k[n]|^2 - N_0}{\mathcal{E}_s}, 0\right)\right]^{\frac{1}{2}} \quad \forall k$

$\hat{\mathbf{s}}^{(k)} = \arg\min_{\mathbf{s}^{(k)}}\|\mathbf{y}^{(k)} - N\hat{h}_{kk}\mathbf{s}^{(k)}\|$

Calculate: $C_{0,k} = \|\mathbf{y}^{(k)} - N\hat{h}_{kk}\hat{\mathbf{s}}^{(k)}\|^2 \quad \forall k$

while $\sum_k f_k \neq 0$ **do**

  Exchange: $\mathbf{s}^{(k)}$, f_k across the DNs

  $i := i + 1$

  for $k = 1 \to K$ **do**

    $\hat{\mathbf{h}}^{(k)} = \frac{1}{N}\mathbf{y}^{(k)}\hat{\mathbf{S}}^{\dagger}$

    $\hat{\mathbf{s}}^{(k)} = \arg\min_{\mathbf{s}^{(k)}}\|\mathbf{y}^{(k)} - N\hat{\mathbf{h}}^{'(k)}\hat{\mathbf{S}}^{'(k)} - N\hat{h}_{kk}\mathbf{s}^{(k)}\|$

    $C_{i,k} = \|\mathbf{y}^{(k)} - N\hat{\mathbf{h}}^{(k)}\hat{\mathbf{S}}\|^2$

    if $C_{i,k} < C_{i-1,k}$ **then**

      $f_k = 1$

    else

      $f_k = 0$

    end if

  end for

end while

This can be solved iteratively by alternately minimizing over $\mathbf{h}^{(k)}$ and $s^{(k)}$ as follows. For minimization over $\mathbf{h}^{(k)}$, we have

$$\hat{\mathbf{h}}^{(k)} = \arg\min_{\mathbf{h}^{(k)}}\|\mathbf{y}^{(k)} - N\mathbf{h}^{(k)}\hat{\mathbf{S}}\|^2. \qquad (67)$$

This can be solved to yield

$$\hat{\mathbf{h}}^{(k)} = \frac{1}{N}\mathbf{y}^{(k)}\hat{\mathbf{S}}^{\dagger}. \qquad (68)$$

This value of $\hat{\mathbf{h}}^{(k)}$ can be then used to update the received symbol estimates at the kth node as

$$\hat{s}_k[n] = \arg\min_{s_k[n]\in\mathcal{S}}|y_k[n] - N\hat{\mathbf{h}}^{'(k)}\hat{\mathbf{s}}^{'(k)}[n] - N\hat{h}_{kk}s_k[n]| \qquad (69)$$

It is easy to find the estimate of $\hat{s}^{(k)}[n]$ from the above, since its complexity is at most linear. The complexity of solving the problem is at most linear in the constellation size. An initial approximation for the diagonal entries of the channel matrix can be obtained using the power method described in [16] as

$$\hat{h}_{kk} \approx \left|\hat{h}_{kk}\right| = \left[\max\left(\frac{\frac{1}{M_d}\sum_{n=1}^{M_d}|y_k[n]|^2 - N_0}{\mathcal{E}_s}, 0\right)\right]^{\frac{1}{2}}, \qquad (70)$$

where the $\max(\cdot,\cdot)$ operation prevents the channel amplitude from taking imaginary values. Using the above estimate, the nodes can assume the initial channel matrix to be diagonal, and form the initial estimate of their data symbols for exchanging with the other nodes over the rate limited channel. A quantized version of the cost function for each node after every channel estimation and data detection step can be augmented with the decoded data symbols being sent over the rate limited communication channel. The nodes can then combine the values of cost functions of all the nodes and arrive at a consensus for stopping the iterations. A pseudo-code for this procedure is provided in Algorithm 1.
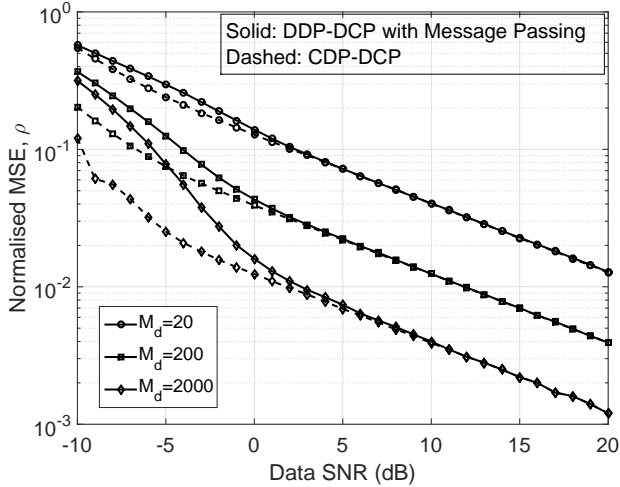
Figure 6. MSE in the channel estimate versus the data SNR for 2 DNs with BPSK and 20 SNs for different number of data symbols per frame.

A. Mean Squared Error (MSE) in Channel Estimation

The channel estimate derived above can also be written as

$$\hat{\mathbf{h}}^{(\mathbf{k})} = \mathbf{h}^{(\mathbf{k})}\mathbf{S}\hat{\mathbf{S}}^{\dagger} + \frac{1}{N}\mathbf{v}^{(k)}\hat{\mathbf{S}}^{\dagger}. \quad (71)$$

Assuming symbol errors to be negligibly small, $\mathbf{S} \approx \hat{\mathbf{S}}$ and therefore $\tilde{\mathbf{h}}^{(k)} \approx \mathbf{v}^{(k)}\mathbf{S}^{\dagger}$. Asuming the symbols across different streams to be uncorrelated, $\mathbf{S}\mathbf{S}^{H} \approx \frac{M_d\mathcal{E}_s}{K}\mathbf{I}_K$, consequently, $\tilde{\mathbf{h}}^{(k)} \approx \frac{K}{NM_d\mathcal{E}_s}\mathbf{v}^{(k)}\mathbf{S}^{H}$.

Now,

$$\tilde{h}_{kl} = \frac{K}{NM_d\mathcal{E}_s}\sum_{n=1}^{M_d} v_k[n]s_l^*[n]. \quad (72)$$

therefore,

$$E[|\tilde{h}_{kl}|^2] = \frac{K^2}{N^2M_d^2\mathcal{E}_s^2}\sum_{m=1}^{M_d}\sum_{n=1}^{M_d} E[v_k[m]s_l[m]v_k^*[n]s_l^*[n]]. \quad (73)$$

Assuming the signal and noise to be independent,

$$\begin{aligned} E[|\tilde{h}_{kl}|^2] &= \frac{K^2}{N^2M_d^2\mathcal{E}_s^2}\sum_{n=1}^{M_d} E[|v_k[n]|^2]E[|s_l[n]|^2] \\ &= \frac{KN_0}{N^2M_d\mathcal{E}_s}. \end{aligned} \quad (74)$$

Hence

$$\frac{E[|\tilde{h}_{kl}|^2]}{E[|h_{kl}|^2]} = \frac{KN_0}{N^3M_d\mathcal{E}_s\Omega}. \quad (75)$$

Fig. 6 plots the ratio $\rho = \frac{\|\mathbf{H}-\hat{\mathbf{H}}\|^2}{\|\hat{\mathbf{H}}\|^2}$ averaged over 10000 independent channel realizations for different number of data symbols under both the data processing architectures for a 2 DN, 20 SN system employing for both CDP-DCP and DDP-DCP. It can be observed that for moderate to high signal SNR the ratio of the MSE to the channel gain reduces linearly with increase in both the data SNR as well as the number of data symbols. However, at lower SNR, the SER is not small enough to be neglected, therefore, the assumption that the $\hat{\mathbf{S}}$ can be approximated by $\mathbf{S}$ does not hold, resulting in a higher MSE.

Also, in general, CDP-DCP based systems are seen to perform better than DDP-DCP based systems, which is as expected.

VI. ERROR PROBABILITY ANALYSIS

In this section, we analyze the probability of error performance for both CDP-DCP and DDP-DCP based systems. Here, we drop the time index of different signals for the sake of simplicity.

A. Symbol Error Rate for CDP-DCP

Considering the received signal as defined in (7), the union bound on the probability of symbol error is

$$P_e \leq \sum_{\mathbf{s}_i \in \mathcal{S}^K} P(\mathbf{s}_i) \sum_{\mathbf{s}_j \in \mathcal{S}^K, j\neq i} P(\mathbf{s}_i \to \mathbf{s}_j) \quad (76)$$

where $P(\mathbf{s}_i \to \mathbf{s}_j)$ is the probability of detecting the transmitted symbol $\mathbf{s}_i$ as $\mathbf{s}_j$, which, in case of an accurate blind channel estimate at the receiver, is given by

$$P(\mathbf{s}_i \to \mathbf{s}_j) = E_{\mathbf{H}}[P(\mathbf{s}_i \to \mathbf{s}_j|\mathbf{H})] \quad (77)$$

where $P(\mathbf{s}_i \to \mathbf{s}_j|\mathbf{H})$ is the pairwise error probability for a given channel realization and is given as

$$P(\mathbf{s}_i \to \mathbf{s}_j|\mathbf{H}) = Q\left(\frac{\|N\mathbf{H}(\mathbf{s}_i - \mathbf{s}_j)\|_2}{\sqrt{N_0}}\right) \quad (78)$$

where $Q(.)$ is the Gaussian-Q function [22]. To obtain expressions for the probability of error, we need to average the above over the distributions of $\mathbf{H}$ and $\hat{\mathbf{H}}$, which is analytically intractable. However, approximate expressions of the probability of symbol error can be derived by using the fact that for a large number of transmitting SNs, due to channel hardening, the off-diagonal terms will be negligible compared to the diagonal terms. Hence, the channel matrix can be approximated as diagonal and the signal received over the kth stream can be written as

$$y_k = Nh_{kk}s_k + v_k. \quad (79)$$

Let us define $P_{e,k}$ as the probability of symbol error for the kth stream. A symbol error occurs when the symbol received over any one of the streams is in error. Therefore, the overall probability of error becomes

$$P_e^{\text{CDP}} = 1 - \prod_{k=1}^{K}(1 - P_{e,k}^{\text{CDP}}). \quad (80)$$

For the entries of the channel matrix being i.i.d. this becomes

$$P_e^{\text{CDP}} = 1 - (1 - P_{e,k}^{\text{CDP}})^K. \quad (81)$$

In (79), while estimating the channel blindly from the unknown data symbols, we assume the channel coefficients to be real positive numbers. However, as discussed in [16], low pilot SNR can cause the channel estimates at different nodes to be erroneous. This results in an increased value of the residual channel phase $\tilde{\theta}_{k,l}$ leading to the phase of h_{kk} being large. Whenever the phase of h_{kk} is large enough to exceed the rotational symmetry of the constellation, catastrophic detection errors occur due to the phase ambiguity at the receiver. This

problem, referred to as *channel corruption*, is common to all blind channel estimation based detection schemes operating on rotationally symmetrical constellations [16]. In the event of a channel corruption, all the received symbols will be decoded incorrectly. The probability of symbol error in the event of a channel corruption at the receiver can therefore be upper bounded by 1. The probability of symbol error over the kth stream can therefore be expressed as

$$P_{e,k}^{\text{CDP}} \approx P_{cc,k} + (1 - P_{cc,k})P_{e,\text{CSIR},k}^{\text{CDP}} \tag{82}$$

where $P_{cc,k}$ represents the probability of channel corruption over the kth stream, and $P_{e,\text{CSIR},k}^{\text{CDP}}$ represents the probability of error over the kth stream with perfect CSI at the receiver. It is safe to assume perfect CSI here, as it has been shown that for a sufficiently large number of data symbols being sent over the channel, a reasonably good estimate of the channel can be had at the receiver when channel corruption does not occur.

1) Derivation of $P_{e,\text{CSIR},k}$ for M-PSK signalling: It was observed in [15] that SNs are generally low cost and employ power amplifiers with small dynamic ranges, consequently making the use of constant modulus constellations such as M-PSK is preferable in these systems. Therefore, in this section we analyze $P_{e,\text{CSIR},k}$ for a DCP based system employing M-PSK modulation, however, the symbol error rate (SER) expressions for QAM constellations are derived in Appendix C. From (79), probability of error for BPSK with perfect CSI at the receiver is [22]

$$P_{e,\text{CSIR},k}^{\text{CDP}} = E\left[Q\left(|h_{kk}|\sqrt{\frac{2N^2\mathcal{E}_s}{KN_0}}\right)\right] \tag{83}$$

and for an M-PSK ($M \geq 4$) constellation, $P_{e,\text{CSIR},k}^{\text{CDP}}$ becomes

$$P_{e,\text{CSIR},k}^{\text{CDP}} \approx 2E\left[Q\left(|h_{kk}|\sqrt{2\frac{N^2\mathcal{E}_s}{KN_0}}\sin\left(\frac{\pi}{M}\right)\right)\right]. \tag{84}$$

The above expectation is over $|h_{kk}|$ whose distribution is not available in closed form. However, similar to the approach followed in [16] we can approximate $h_{kk} = \sum_{l=1}^{N} \alpha_{k,l}$ as a Nakagami-m distributed r.v. [23] with its parameters m_R and $\bar{\gamma}_R$ chosen using the moment matching method as [24], [25]

$$m_R = \left\lceil \frac{E^2[|h_{kk}|^2]}{\text{var}(|h_{kk}|^2)} \right\rceil \tag{85}$$

$$\bar{\gamma}_{R,\text{BPSK}} = \frac{2N^2\mathcal{E}_s}{KN_0}E[|h_{kk}|^2] \tag{86}$$

$$\bar{\gamma}_{R,\text{MPSK}} = \frac{2N^2\mathcal{E}_s\sin^2\left(\frac{\pi}{M}\right)}{KN_0}E[|h_{kk}|^2]. \tag{87}$$

In the above equations, the estimated Nakagami parameter m_R is rounded (denoted by $\lceil . \rceil$) to the nearest integer for simplicity. Using the results derived in Section II and [16], $P_{e,\text{CSIR},k}^{\text{CDP}}$ can be obtained for BPSK as [26]

$$P_{e,\text{CSIR},k}^{\text{CDP}} = \frac{\phi(\bar{\gamma}_{R,\text{BPSK}}, m_R)}{2\sqrt{\pi}}\frac{\Gamma(m_R + \frac{1}{2})}{\Gamma m_R + 1}$$
$${}_2F_1\left(1, m_R + \frac{1}{2}; m_R + 1; \frac{2m_R}{2m_R + \bar{\gamma}_{R,\text{BPSK}}}\right). \tag{88}$$

and for M-PSK ($M \geq 4$) as

$$P_{e,\text{CSIR},k}^{\text{CDP}} \approx \frac{\phi(\bar{\gamma}_{R,\text{MPSK}}, m_R)}{\sqrt{\pi}}\frac{\Gamma(m_R + \frac{1}{2})}{\Gamma m_R + 1}$$
$${}_2F_1\left(1, m_R + \frac{1}{2}; m_R + 1; \frac{2m_R}{2m_R + \bar{\gamma}_{R,\text{MPSK}}}\right). \tag{89}$$

In the above equation,

$$\phi(\bar{\gamma}_{R,t}, m_R) \triangleq \left(1 + \frac{\bar{\gamma}_{R,t}}{2m_R}\right)^{-m_R - \frac{1}{2}} \tag{90}$$

for both BPSK and M-PSK, $\Gamma(n)$ is the gamma function, and ${}_2F_1(a, b; c; d)$ is the Gauss hypergeometric function [27].

2) Derivation of $P_{cc,k}$: If each sensor node employs the constellation $\mathcal{S}$ with a rotational symmetry φ, for M-PSK $\varphi = 2\pi/M$, channel corruption occurs whenever $\angle h_{kk} > \frac{\varphi}{2}$. The probability of channel corruption hence becomes

$$P_{cc,k} = \Pr\left\{|\angle h_{kk}| > \frac{\varphi}{2}\right\}. \tag{91}$$

It is shown in Appendix B that the above can be expressed as

$$P_{cc,k} = Q\left(\frac{\mu_R}{\sigma_R}\right) + 2Q\left(\frac{\mu_R}{\sqrt{\frac{\sigma_I^2}{\tan^2\frac{\varphi}{2}} + \sigma_R^2}}\right)$$
$$\times \left(1 - Q\left(\frac{\mu_R}{\sigma_R}\right)\right)\mathbb{1}_{\{\varphi < \pi\}} \tag{92}$$

where

$$\mu_R = \sqrt{\frac{\Omega\pi}{4}}\sqrt{\frac{\xi\Omega}{1 + \xi\Omega}}$$
$$\sigma_R^2 = \frac{\Omega(2 + (4 - \pi)\xi\Omega)}{N(1 + \xi\Omega)}$$
$$\sigma_I^2 = \frac{\Omega}{2N(1 + \xi\Omega)}. \tag{93}$$

Using the expression for $P_{e,\text{CSIR},k}^{\text{CDP}}$ from (83)/(84) and P_{cc} from (92), the symbol error probability for CDP-DCP can now be computed in closed form.

B. Symbol Error Rate for DDP-DCP

In the case of DDP-DCP, a symbol error occurs if the symbol transmitted on any of the streams is decoded in error.

Looking at (43), a symbol error can be caused either due to channel corruption or due to the additive noise and interference. The probability of error is therefore approximated as a sum of the probability of channel corruption and that of an error due to noise and interference in the event of no channel corruption, and can be written as

$$P_{e,k}^{\text{DDP}} \approx P_{cc,k} + (1 - P_{cc,k})P_{I,k}, \tag{94}$$

where $P_{cc,k}$ is the probability of channel corruption for the kth stream and has been derived in the previous subsection, and $P_{I,k}$ is the probability of symbol error due to additive noise and interference.

As discussed previously, the average interference power can be expressed as $E\left[|\tilde{z}_k[n]|^2\right] = \mu N\frac{(K-1)\Omega\mathcal{E}_s}{K}$. Here, the

interference mitigation factor, μ, is dependent on the performance of the message passing based blind channel estimation algorithm. For example, when there is no communication between the SNs, and therefore no interference mitigation, $\mu = 1$. In case of perfect interference mitigation, i.e., when the symbols and channels on the interfering streams are perfectly known at each DN, $\mu = 0$. The noise plus interference power therefore becomes $\mu(K-1)\Omega\mathcal{E}_s/K + N_0$. Considering BPSK signaling by the sensor nodes, $P_{I,k}$ can be expressed as

$$P_{I,k} = E\left[Q\left(|h_{kk}|\sqrt{\frac{2N^2\mathcal{E}_s}{\mu N(K-1)\Omega\mathcal{E}_s + KN_0}}\right)\right], \quad (95)$$

and for M-PSK signaling this becomes

$$P_{I,k} = 2E\left[Q\left(|h_{kk}|\sqrt{\frac{2N^2\mathcal{E}_s}{\mu N(K-1)\Omega\mathcal{E}_s + KN_0}}\sin\left(\frac{\pi}{M}\right)\right)\right]. \quad (96)$$

This can again be solved using a Nakagami-m approximation for h_{kk} with the parameter $\bar{\gamma}_R$ being given as

$$\bar{\gamma}_{R,\text{BPSK}} = \frac{2N^2\mathcal{E}_s E[|h_{kk}|^2]}{\mu N(K-1)\Omega\mathcal{E}_s + KN_0} \quad (97)$$

$$\bar{\gamma}_{R,\text{MPSK}} = \frac{2N^2\mathcal{E}_s \sin^2\left(\frac{\pi}{M}\right)E[|h_{kk}|^2]}{\mu N(K-1)\Omega\mathcal{E}_s + KN_0}. \quad (98)$$

Following this, (85) and (88) can be used to calculate $P_{I,k}^{\text{DDP}}$, which can be used, along with the probability of channel corruption, to compute $P_{e,k}^{\text{DDP}}$ in closed form.

VII. SIMULATION RESULTS

In this section, we use numerical results based on Monte Carlo simulations to corroborate the analytical expressions derived previously and to demonstrate the performance of various channel estimation and data detection schemes.

Similar to the model used in [16], we assume that 10 training symbols are sent from each DN to the SNs followed by M_d data symbols from the SNs to the DNs using DCP based on the estimated channel phase. Simulations are then carried out for different values of pilot and data SNR, different numbers of SNs and DNs, etc. DCP uses reverse link training, that is, the pilots are transmitted by the DNs, which are connected to the mains and can transmit at higher power compared to the power-starved SNs. In view of this, we assume the pilot SNR (ξ) to be 10 dB, unless specified otherwise. Also, the total power radiated from the SNs is kept fixed, so as to keep the comparison fair. The SER and the MSE in channel estimation are obtained by averaging over $20,000$ independent channel realizations.

In Fig. 7, the performance of CDP-DCP based on different blind channel estimation techniques are compared against ideal DCP and the derived theoretical approximations. It is seen that the performance of DCP based on the proposed iterative blind channel estimation technique closely follows the performance of ideal DCP and is in agreement with the theoretical approximations. It is also observed that iterative blind channel estimation based DCP results in a performance improvement of nearly 3 dB over the covariance method based DCP for a two DN QPSK system at an SER of 10^{-3}.
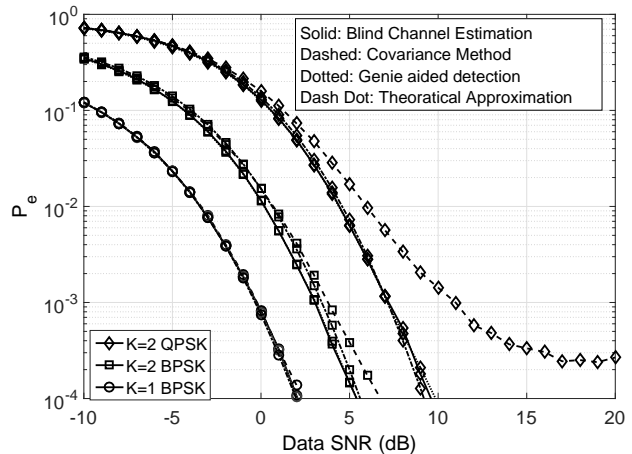

Figure 7. Probability of symbol error versus the data SNR for different communication setups for 10 SNs with $K = 1, 2$ DNs using CDP-DCP.
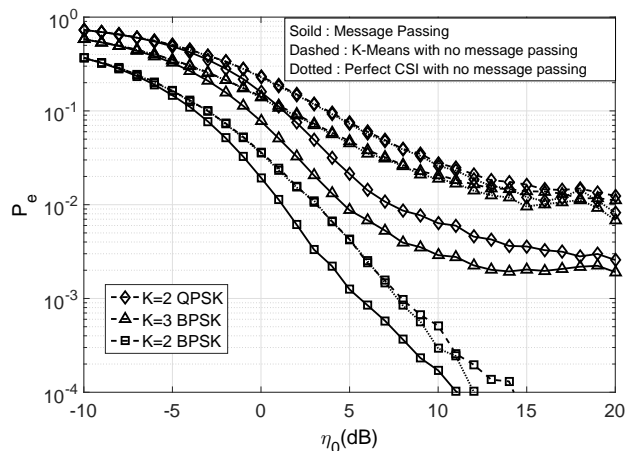

Figure 8. Probability of symbol error versus the data SNR (η_0) for different number of DNs and 10 SNs.

In Fig. 8, the performance of DDP-DCP employing message passing based blind channel estimation is compared against streamwise decoding without message passing with perfect and estimated CSI at the receiver. In case of streamwise decoding without message passing, the K-means based blind channel estimation and decoding method proposed in [16] is employed, and is depicted by dashed line curves in the figure. The dotted lines in the figure represent the case where the diagonal entries of the channel matrix are perfectly known at the receiver, however there is no sharing of messages among the DNs, and therefore no interference cancellation. Message passing is seen to significantly improve the performance of the DDP-DCP system in all cases. It is observed that for a two DN QPSK system, the probability of error floor is almost one order of magnitude lower than that for systems without message passing.

Fig. 9 compares the performance of CDP against DDP schemes with and without message passing for 2 DNs and 10 SNs. As expected, the CDP scheme performs better than DDP with message passing which in turn outperforms DDP
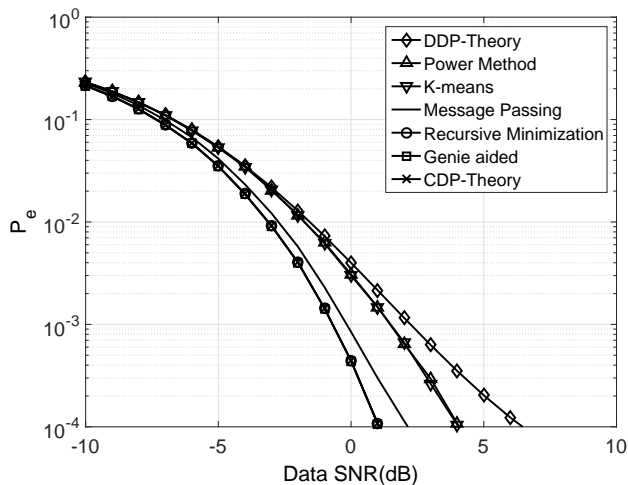
Figure 9.   Probability of symbol error versus data SNR for 2 DNs employing BPSK at pilot SNR = 10 dB for $N = 20$ SNs and different reception schemes.
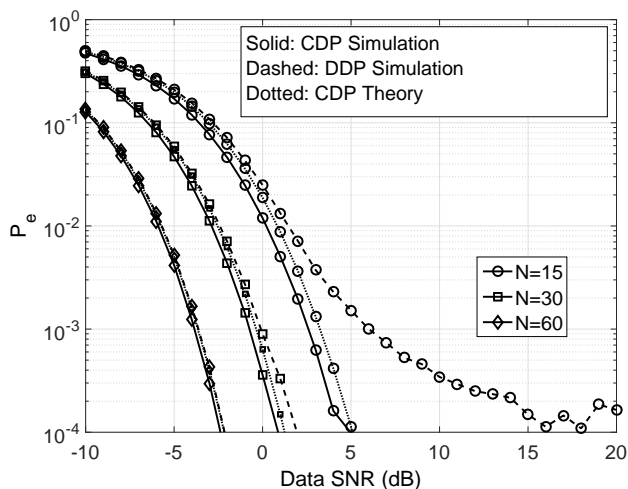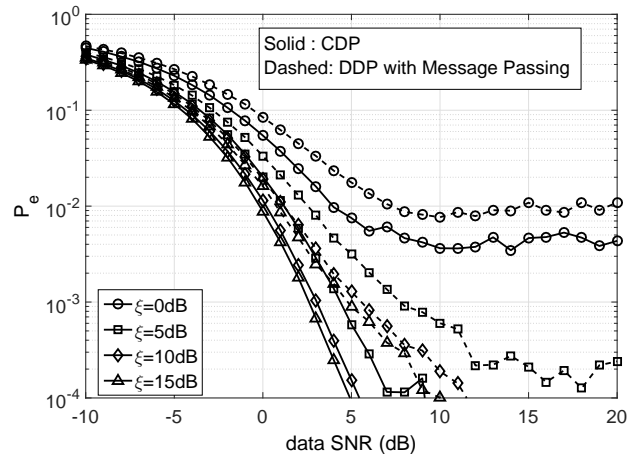

Figure 11.   Probability of symbol error versus the data SNR for 2 DNs with BPSK and 10 sensor nodes at different pilot SNR.

Figure 10.   Probability of symbol error versus the SNR for 3 DNs employing BPSK at pilot SNR = 10 dB for different number of sensor nodes.
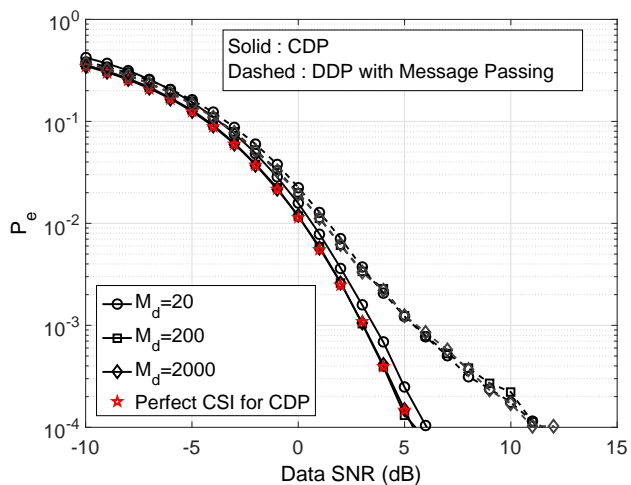

Figure 12.   Probability of symbol error versus the data SNR for 2 DNs with BPSK and 10 SNs for different number of data symbols.

without message passing. In the above figure, all the curves marked with the caption DDP refer to DDP without message passing. The gap between the theoretical and actual values of DDP without message passing can be attributed to the fact that the theoretical error performance is computed approximating the interference as Gaussian noise, which is somewhat inaccurate when there is only one interfering stream and BPSK modulation is employed.

Fig. 10 compares the performance of a three DN BPSK based system for different number of sensor nodes. The performance of the blind channel estimation based system is again found to be close to the theoretical approximation. It can be observed that the theoretical approximates get closer to the true error performance as the number of SNs increases and consequently the channel hardens. Increasing the number of sensor nodes from 15 to 60 is observed to result in an data SNR gain of approximately 8 dB at an error rate of 10^{-3}.

The performance of CDP-DCP and DDP-DCP is compared

for different pilot SNR (ξ) in Fig. 11. CDP-DCP is again seen to outperform DDP-DCP with a margin of more than 2 dB for a symbol error rate of 10^{-3} at a pilot SNR of 15 dB.

In Fig. 12 the symbol error rates for CDP and DDP schemes are plotted against the data SNR for different number of uplink data symbols per frame. The dependence of symbol error rates on the number of data symbols arises due to the fact that the quality of the channel estimate depends on the number of data symbols. It is observed that in CDP-DCP, 200 data symbols are sufficient to obtain a performance close to perfect CSI at the DNs.

In Fig. 13, the symbol error rates for CDP and message passing based DDP schemes are plotted against the data SNR for i.n.d. channel coefficients. The distributions of the channel coefficients are same as those in Fig. 4. The plots for both CDP and DDP systems are observed to closely follow the derived theory for the i.i.d. case, thus showing that the results derived in this work extend well to a system with i.n.d. channel coefficients.
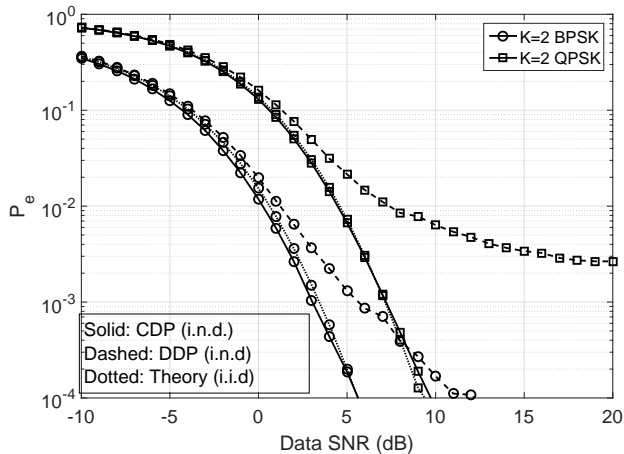
Figure 13. Probability of symbol error verus the data SNR for different communication setups for 10 SNs with $K=2$ DNs under both CDP and DDP for i.n.d. distributed channel coefficients.

VIII. CONCLUSIONS

In this work, we showed that using multiple DNs improves the achievable rates for a DCP based system both for centralized as well as distributed processing. We then proposed a blind channel estimation algorithm to estimate the effective DCP channel for the CDP-DCP case. A message passing version of this algorithm was then developed for use in the DDP-DCP case. We developed approximate expressions to analyze the performance of the proposed systems. These expressions were then verified using an extensive simulation study. It was shown through simulations that the proposed blind channel estimation algorithm can perform almost as good as a detector with perfect CSI at the DNs. Hence uplink pilots are not necessary. Future work could consider design and analysis of diversity reception techniques for the proposed system.

APPENDIX A
BOUND ON THE MEAN SQUARED SYMBOL ERROR

The symbol error $\tilde{s}_k$ is defined as $\tilde{s}_k = s_k - \hat{s}_k$ for $s_k, \hat{s}_k \in \mathcal{S}$. The mean squared value of $\tilde{s}_k$ becomes

$$E[|\tilde{s}_k|^2] = \sum_{s_k \in \mathcal{S}} \sum_{\hat{s}_k \in \mathcal{S}} P(s_k) P\{s_k \to \hat{s}_k\}[|s_k - \hat{s}_k|^2]. \quad (99)$$

Considering all the symbols to be equally likely, the above can be written as

$$E[|\tilde{s}_k|^2] = \frac{1}{|\mathcal{S}|} \sum_{s_k \in \mathcal{S}} \sum_{\hat{s}_k \in \mathcal{S}, s_k \neq \hat{s}_k} P\{s_k \to \hat{s}_k\}[|s_k - \hat{s}_k|^2]. \quad (100)$$

Defining $P_{e,\max}$ as the probability of mis-detecting a symbol as one of its adjacent symbols, $P(s_k \to \hat{s}_k) \leq P_{e,\max}$. Also, for constant envelope signal constellations, we have

$$|s_k - \hat{s}_k|^2 \leq 4\frac{\mathcal{E}_s}{K}. \quad (101)$$

Using these, (100) becomes

$$
\begin{aligned}
E[|\tilde{s}_k|^2] &\leq \frac{1}{|S|} \sum_{s_k \in \mathcal{S}} \sum_{\hat{s}_k \in \mathcal{S}, \hat{s}_k \neq s_k} P_{e,\max} 4\frac{\mathcal{E}_s}{K} \\
&= 4(|\mathcal{S}| - 1)P_{e,\max}\frac{\mathcal{E}_s}{K}.
\end{aligned}
\quad (102)
$$

Hence,

$$\frac{KE[|\tilde{s}_k|^2]}{\mathcal{E}_s} \leq 4(|\mathcal{S}| - 1)P_{e,\max}. \quad (103)$$

The above is is less than unity when $P_{e,\max} < \frac{1}{4(|\mathcal{S}|-1)}$, which will be the case for a well designed system.

APPENDIX B
DERIVATION OF $P_{cc,k}$

Considering the fact that the maximum rotational symmetry of a constellation is π, and therefore, a channel corruption will result whenever h_{kk} lies in the right half plane. Based on this, we can split (91) as

$$
\begin{aligned}
P_{cc,k} = &\Pr\left\{\measuredangle|h_{kk}| > \frac{\pi}{2}\right\} \\
&+ \left(\Pr\left\{\measuredangle|h_{kk}| > \frac{\varphi}{2} \,\Big|\, \measuredangle|h_{kk}| < \frac{\pi}{2}\right\}\right) \\
&\left(1 - \Pr\left\{\measuredangle|h_{kk}| > \frac{\pi}{2}\right\}\right)\mathbb{1}_{\{\varphi < \pi\}}. \quad (104)
\end{aligned}
$$

Here, $\mathbb{1}_{\{A\}}$ is the indicator function that evaluates to 1 when the event A is true, and evaluates to 0 when A is false.

Now, as $\measuredangle h_{kk} = \tan^{-1}\left(\frac{\Im\{h_{kk}\}}{\Re\{h_{kk}\}}\right)$, the above equation can be rewritten as

$$
\begin{aligned}
P_{cc,k} = &\Pr\{\Re\{h_{kk}\} < 0\} \\
&+ 2\left(\Pr\left\{\Im\{h_{kk}\} > \tan\left(\frac{\varphi}{2}\right)\Re\{h_{kk}\}\right\}\right) \\
&(1 - \Pr\{\Re\{h_{kk}\} < 0\})\mathbb{1}_{\{\varphi < \pi\}}. \quad (105)
\end{aligned}
$$

Using the fact that both $\Re\{h_{kk}\}$ and $\Im\{h_{kk}\}$ are real valued Gaussian r.v.s, $\Pr\left\{\Im\{h_{kk}\} > \tan\left(\frac{\varphi}{2}\right)\Re\{h_{kk}\}\right\}$ can be expressed as

$$\Pr\left\{\measuredangle h_{kk} \geq \frac{\varphi}{2}\right\} = Q\left(\frac{\mu_{R,k}}{\sqrt{\frac{\sigma_{I,k}^2}{\tan^2\frac{\varphi}{2}} + \sigma_{R,k}^2}}\right) \quad (106)$$

where $\mu_{R,k} = E[\Re\{h_{kk}\}]$, $\sigma_{R,k}^2 = \text{var}(\Re\{h_{kk}\})$ and $\sigma_{I,k}^2 = \text{var}(\Im\{h_{kk}\})$. Using (11) and (13), we can write

$$
\begin{aligned}
\mu_R &= \sqrt{\frac{\Omega\pi}{4}}\sqrt{\frac{\xi\Omega}{1 + \xi\Omega}} \\
\sigma_R^2 &= \frac{\Omega(2 + (4 - \pi)\xi\Omega)}{N(1 + \xi\Omega)} \\
\sigma_I^2 &= \frac{\Omega}{2N(1 + \xi\Omega)}.
\end{aligned}
\quad (107)
$$

It is shown in [15] that

$$\Pr\{\Re\{h_{kk}\} < 0\} = Q\left(\frac{\mu_R}{\sigma_R}\right). \quad (108)$$

These expressions can be substituted in (91) to obtain (92).

APPENDIX C

SYMBOL ERROR RATE FOR QAM CONSTELLATIONS

From (79), the probability of error for the M-PAM constellation with perfect CSI at the receiver and CDP-DCP is given by [22]

$$P_{e,\text{CSIR},k}^{\text{CDP,PAM}} = E\left[\frac{2(M-1)}{M}Q\left(\sqrt{\frac{6\mathcal{E}_s}{(M^2-1)N_0}}|h_{kk}|\right)\right] \tag{109}$$

This can again be solved using a Nakagami-m approximation for the argument of the Q-function, to obtain

$$P_{e,\text{CSIR},k}^{\text{CDP,PAM}} = \frac{M-1}{M}\frac{\phi(\bar{\gamma}_{R,\text{PAM}},m_R)}{2\sqrt{\pi}}\frac{\Gamma(m_R+\frac{1}{2})}{\Gamma(m_R+1)}$$
$$\,_2F_1\left(1,m_R+\frac{1}{2};m_R+1;\frac{2m_R}{2m_R+\bar{\gamma}_{R,\text{PAM}}}\right). \tag{110}$$

where

$$\bar{\gamma}_{R,\text{PAM}} = \frac{6N^2\mathcal{E}_s}{K(M^2-1)N_0}E[|h_{kk}|^2], \tag{111}$$

and $\phi(\bar{\gamma}_{R,\text{PAM}},m_R)$ can be calculated using (90). For DDP, the above expressions modify to

$$P_{I,k}^{\text{DDP,PAM}} = E\left[\frac{2(M-1)}{M}\right.$$
$$\left. Q\left(\sqrt{\frac{6\mathcal{E}_s}{(M^2-1)(\mu N(K-1)\Omega\mathcal{E}_s+KN_0)}}|h_{kk}|\right)\right] \tag{112}$$

This can also be calculated using the Nakagami-m approximation with a form similar to (110), and

$$\bar{\gamma}_{R,\text{PAM}} = \frac{6N^2\mathcal{E}_s}{(M^2-1)(\mu N(K-1)\Omega\mathcal{E}_s+KN_0)}E[|h_{kk}|^2]. \tag{113}$$

Now, since the QAM constellation can be viewed as a superposition of two orthogonal PAM constellations, therefore,

$$P_{e,\text{CSIR},k}^{\text{CDP,QAM}} = 2P_{e,\text{CSIR},k}^{\text{CDP,PAM}} - (P_{e,\text{CSIR},k}^{\text{CDP,PAM}})^2. \tag{114}$$

The overall probabilities of error for PAM and QAM become,

$$P_{e,k}^{\text{CDP,PAM}} = P_{cc,k}^{\text{PAM}} + (1-P_{cc,k})P_{e,\text{CSIR},k}^{\text{CDP,PAM}} \tag{115}$$

$$P_{e,k}^{\text{CDP,QAM}} = P_{cc,k}^{\text{QAM}} + (1-P_{cc,k})P_{e,\text{CSIR},k}^{\text{CDP,QAM}} \tag{116}$$

where $P_{cc,k}^{\text{PAM}}$ and $P_{cc,k}^{\text{QAM}}$ can be calculated using the facts that the rotational symmetries of PAM and QAM are $\phi = \frac{\pi}{2}$, and $\phi = \frac{\pi}{4}$, respectively.

REFERENCES

[1] R. Chopra, C. R. Murthy, and R. Annavajjala, "Multi-stream distributed co-phasing: Design and analysis," in *Proc. SPAWC*, pp. 1–6, July 2016.

[2] J. Chamberland and V. Veeravalli, "Wireless sensors in distributed detection applications," *IEEE Signal Process. Mag.*, vol. 24, pp. 16–25, May 2007.

[3] Y.-S. Tu and G. Pottie, "Coherent cooperative transmission from multiple adjacent antennas to a distant stationary antenna through AWGN channels," in *Proc. VTC (Spring)*, pp. 130–134, May 2002.

[4] R. Mudumbai, D. Brown, U. Madhow, and H. Poor, "Distributed transmit beamforming: challenges and recent progress," *IEEE Commun. Mag.*, vol. 47, pp. 102–110, Feb. 2009.

[5] R. Mudumbai, G. Barriac, and U. Madhow, "On the feasibility of distributed beamforming in wireless networks," *IEEE Trans. Wireless Commun.*, vol. 6, pp. 1754–1763, May 2007.

[6] R. Mudumbai, J. Hespanha, U. Madhow, and G. Barriac, "Distributed transmit beamforming using feedback control," *IEEE Trans. Inf. Theory*, vol. 56, pp. 411–426, Jan. 2010.

[7] M. M. U. Rahman, R. Mudumbai, and S. Dasgupta, "Consensus based carrier synchronization in a two node networks," in *18th IFAC World Congress*, pp. 10038–10043, June 2011.

[8] S. Zhou and G. Giannakis, "How accurate channel prediction needs to be for transmit-beamforming with adaptive modulation over Rayleigh MIMO channels?," *IEEE Trans. Wireless Commun.*, vol. 3, pp. 1285–1294, July 2004.

[9] P. Fertl, A. Hottinen, and G. Matz, "Perturbation-based distributed beamforming for wireless relay networks," in *Proc. Globecom*, pp. 1–5, Nov. 2008.

[10] C. Lin, V. Veeravalli, and S. Meyn, "A random search framework for convergence analysis of distributed beamforming with feedback," *IEEE Trans. Inf. Theory*, vol. 56, pp. 6133–6141, Dec. 2010.

[11] Y. Jing and H. Jafarkhani, "Network beamforming using relays with perfect channel information," *IEEE Trans. Inf. Theory*, vol. 55, pp. 2499–2517, June 2009.

[12] A. Ekbal and J. Cioffi, "Distributed transmit beamforming in cellular networks - a convex optimization perspective," in *Proc. ICC*, vol. 4, pp. 2690–2694 Vol. 4, May 2005.

[13] M. K. Banavar, A. D. Smith, C. Tepedelenlioglu, and A. Spanias, "On the effectiveness of multiple antennas in distributed detection over fading macs," *IEEE Trans. Wireless Commun.*, vol. 11, pp. 1744–1752, May 2012.

[14] D. Ciuonzo, G. Romano, and P. Salvo Rossi, "Channel-aware decision fusion in distributed MIMO wireless sensor networks: Decode-and-fuse vs. decode-then-fuse," *IEEE Trans. Wireless Commun.*, vol. 11, pp. 2976–2985, Aug. 2012.

[15] K. Chaythanya, R. Annavajjala, and C. Murthy, "Comparative analysis of pilot-assisted distributed cophasing approaches in wireless sensor networks," *IEEE Trans. Signal Process.*, vol. 59, pp. 3722–3737, Aug. 2011.

[16] A. Manesh, C. Murthy, and R. Annavajjala, "Physical layer data fusion via distributed co-phasing with general signal constellations," *IEEE Trans. Signal Process.*, vol. 63, pp. 4660–4672, Sept. 2015.

[17] T. M. Cover and J. A. Thomas, *Elements of Information Theory (Wiley Series in Telecommunications and Signal Processing)*. Wiley-Interscience, 2006.

[18] A. Paulraj, R. Nabar, and D. Gore, *Introduction to Space-Time Wireless Communications*. New York, NY, USA: Cambridge University Press, 1st ed., 2008.

[19] L. Tong and S. Perreau, "Multichannel blind identification: from subspace to maximum likelihood methods," *Proc. IEEE*, vol. 86, pp. 1951–1968, Oct. 1998.

[20] H. H. Zeng and L. Tong, "Blind channel estimation using the second-order statistics: algorithms," *IEEE Trans. Signal Process.*, vol. 45, pp. 1919–1930, Aug. 1997.

[21] T. Narasimhan and A. Chockalingam, "Channel hardening-exploiting message passing (CHEMP) receiver in large-scale MIMO systems," *IEEE J. Sel. Topics Signal Process.*, vol. 8, pp. 847–860, Oct. 2014.

[22] S. Haykin, *Digital Communication Systems*. Wiley Publishing, 1st ed., 2013.

[23] M. Schwartz, W. R. Bennett, and S. Stein, *Communication systems and techniques*. Inter-university electronics series, New York: McGraw-Hill, 1966.

[24] P. K. Vitthaladevuni and M. S. Alouini, "A recursive algorithm for the exact BER computation of generalized hierarchical QAM constellations," *IEEE Trans. Inf. Theory*, vol. 49, pp. 297–307, Jan. 2003.

[25] N. Beaulieu and C. Cheng, "Efficient Nakagami-m fading channel simulation," *IEEE Trans. Veh. Technol.*, vol. 54, pp. 413–424, Mar. 2005.

[26] H. Shin and J. H. Lee, "On the error probability of binary and M-ary signals in nakagami-m fading channels," *IEEE Trans. Commun.*, vol. 52, pp. 536–539, Apr. 2004.

[27] F. Beukers, "Gauss' hypergeometric function," in *Arithmetic and Geometry Around Hypergeometric Functions* (R.-P. Holzapfel, A. Uludağ, and M. Yoshida, eds.), vol. 260 of *Progress in Mathematics*, pp. 23–42, Birkhäuser Basel, 2007.